AIAA Aviation Forum and ASCEND co-located Conference Proceedings
29 July - 2 August 2024, Las Vegas, Nevada
AIAA AVIATION FORUM AND ASCEND 2024
10.2514/6.2024-4489

Testing for slipperiness: Review of Flight Test Activities on Wet Runways using a Cessna Citation 550 and Dassault Falcon 2000

Gerard W.H. van Es* and Vincent J.F. de Vries†
Netherlands Aerospace Centre NLR, Amsterdam, 1059 CM, The Netherlands

An overview is given of the flight test activities of the ongoing runway micro texture project conducted by Netherlands Aerospace Centre and its partners the German Aerospace Centre and Engineering Sciences Data Unit for the European Union Aviation Safety Agency. The test locations, flight test aircraft, test equipment, and flight test procedures are described. The post processing of the data collected during the flight test with Cessna Citation C550 and the Dassault Falcon 2000 on wet runways is discussed in some detail. Some preliminary results in terms of braking friction levels as function of ground speed are presented for several test locations. Results from testing the two test aircraft on wet runway at several airports are reviewed.

I. Nomenclature

W	=	Weight
g	=	Acceleration due to gravity
a_x	=	Longitudinal acceleration along runway
T_{idle}	=	Idle engine thrust
D	=	Aerodynamic drag
L	=	Aerodynamic lift
γ	=	Runway slope (positive uphill)
$\mu_{b\_a/c}$	=	Aircraft braking friction coefficient
$a_{x\ body}$	=	Acceleration parallel to the aircraft axis
$a_{z\ body}$	=	Acceleration perpendicular to the aircraft axis
θ	=	Aircraft pitch angle
N_m	=	Normal load on main gear wheels
μ_b	=	Main gear wheel braking friction coefficient
μ_r	=	Rolling friction coefficient

II. Introduction

The European Union Aviation Safety Agency (EASA) (Ref. [1]) categorises runway excursions as one of the top two risk areas for large aircraft and business aircraft. In a runway excursion a pilot is either not able to stop on the runway and overruns it or has control problems and veers off the side of the runway. It represents one of the most serious risks in aviation and is one of the most economically significant safety events. The slipperiness of the runway is one the most important contributing factors in runway excursions. A runway can become slippery when it is wet or contaminated with e.g. snow or ice. The ground distance needed to stop an aircraft during landing or an aborted takeoff will increase compared to a dry runway under these conditions. Controlling an aircraft on a slippery runway under crosswind conditions is also more difficult than on a dry runway.

* Principle Consultant, Flight Operations & Safety department.
† R&D Engineer, Flight Testing department.

Over the years, a number of runway overrun accidents and incidents have occurred after the aircraft landed on a wet runway. An analysis of the aircraft stopping performance showed that the wheel braking friction coefficient achieved during the landing roll was significantly less than predicted by industry-accepted models provided in the applicable certification specifications such as EASA CS 25.109, or assumed in the wet-runway landing distance advisory data provided in the manufacturers' aircraft flight manuals. In these overrun accidents and incidents the runway was just wet (not flooded), and was not classified as 'slippery wet' by the airport. All involved aircraft had fully operative brakes and anti-skid systems. Given the conditions and circumstances it is believed that deficiencies in the runway micro texture have resulted in the lower wheel braking friction levels. Micro texture refers to the fine scale roughness contributed by small individual aggregate particles on pavement surfaces. A good sharp micro texture pavement (like gritty sand paper) can puncture and displace the thin water film trapped in the tyre footprint and thus prevent or greatly alleviate the build-up of viscous water pressures that create this type of friction loss.

At this moment there are no acceptable methods for assessing the runway micro texture directly. Many overrun occurrences could have been avoided if the braking performance had matched that specified in certification standards, or if the crew had been informed in a timely manner that the runway was slippery wet.

The recently published Global Action Plan for the Prevention of Runway Excursions (GAPPRE) has emphasized the importance of assessing the runway micro texture characteristics accurately to reduce the number of runway excursions. Also the introduction of the runway condition assessment matrix used by both pilots and airports has further stressed the importance to identify runways that are slippery when wet.

In recent years high-resolution surface laser scanners have been used to assess the micro texture of road pavements. Runways have also been explored but to a lesser extent. Initial results on runways are promising and indicate that these laser scanners could help to identify poor micro textured runways surfaces and hence 'slippery wet' runways. However, more research is needed to define a practical application and to validate the results obtained. Correlation with flight test results is for instance needed and also the development of threshold values for micro texture characteristics of a runway is required. EASA has started a research effort intended to address the risk of overruns caused by deficiencies in runway micro texture, and explore the use of laser-scanning to establish suitable thresholds for runway surfaces which define when a runway is slippery when wet. This paper describes some of the preliminary results of this project. The project is funded from the European Union's Horizon Europe research and innovation programme. This research project is conducted by the Royal Netherlands Aerospace Centre (NLR) together with the German Aerospace Centre (DLR) and Engineering Sciences Data Unit (ESDU).

The EASA research project covers several elements with one part concerning an extensive test campaign. Two fully instrumented aircraft have been tested on artificially wetted runway pavements that vary in texture and construction, along with measurements taken using a high-resolution laser surface scanner. Wheel braking friction characteristics will be derived from the flight tests. Using these flight test derived friction data a parameter that characterises the micro texture of the runway will be deduced. The correlation found between microtextural characteristics obtained with laser scanner and micro texture characteristic from the flight tests data will be finally used to define thresholds for a slippery wet runway. The present paper discuss the results obtained in the flight test campaign. Details about the execution of the flight test themselves, the preparations taken, description of the different test locations, the post processing and some results are presented and discussed.

III. Test aircraft

Two test aircraft were used in the flight test program, a Cessna Citation C550 and a Dassault Falcon 2000LX. Both test aircraft are shown in Fig. 1. The Cessna Citation is a small sized business jet and the Falcon 2000 is a medium sized business jet.

Originally designed for executive travel, the NLR Cessna Citation C550 test aircraft (registration PH-LAB) has been extensively modified by NLR to serve as a versatile airborne research platform. The basic crew consist of two pilots. When empty, a maximum of eight observers can be seated in the cabin. It has two Pratt & Whitney JT15D-4 turbofan engines. The Citation C550 has a single wheel type VII 22x8.00-10 (bias-ply) main landing gear. New wheel brake units and new (unworn) tires were installed on the main gear prior to testing. The main gear tire inflation pressure was 115 psi and maintained within ±5 psi throughout the course of the test program. Tire tread depths were above 6 mm during all tests.

The Falcon 2000LX is a transcontinental twin-engine business jet. The Falcon 2000LX is a representative aircraft type for modern, medium-large business jets. The basic crew consist of two pilots. The aircraft has two Pratt & Whitney PW308C turbofan engines. The Falcon 2000 has a dual wheel 26x6.6R14 (radial-belted) main landing gear. Relatively new tires were installed on the main gear prior to testing. The main gear tire inflation pressure was 225 psi and maintained within ±5 psi throughout the course of the test program. Tire tread depths were above 6 mm during all tests.

Fig. 1: aircraft used in the flight test program

IV. Flight test locations

The selection of different test sites used in this study was based on the variety of runway surface types available; necessary support equipment and personnel; low traffic volumes; and typical weather conditions (wind and precipitation). The primary test sites were Twente Airport, Braunschweig Airport, Cochstedt Airport, and NASA Wallops Flight Facility. The first three airports are located in Europe, the last airport is in the United States.

Twente Airport is located to the east of the Netherlands and was a former military base. Currently it is used for flight testing, business jet operations and general aviation flights. Twente Airport has one runway 05/23 that is 45 m wide and 2400 m long with a uniform, high-macro textured, chip seal surface (Possehl antiskid). Braunschweig Airport (also known as Braunschweig-Wolfsburg Airport) is located in Germany. It is mainly used by business jet operators, air taxi, general aviation and some charter flights. Braunschweig Airport has one runway 08/26 that is 45 m wide and 2300 m long with a uniform, medium-macro textured, asphalt surface. Cochstedt Airport is located in Germany. It is operated and owned by DLR. It is mainly used for (drone) flight testing. The single runway 08/26 is 2,500 m long and 45 m wide with a uniform, medium-macro textured, asphalt surface. The taxiway of Cochstedt Airport was also used in the flight testing which has a low-macro textured, brushed concrete surface. The Wallops Flight Facility is located on the East Coast of the United States and is operated by NASA. It is mainly used for flight testing and training. The airport has three runways. The three-runway layout at Wallops Flight Facility is shown in Fig. 2. Runway 17/35 was not used in this study. Runway 10/28 is 60 m wide and 2,400 m long with a uniform, medium-macrotexture, slurry-seal asphalt surface. Runway 04/22, also referred to as the landing research runway, is 45 m wide and 2,600 m long. The specially constructed level (no crown) test section, located on runway 04/22 some 707 m from the threshold of runway 22, consists of two grooved and two non-grooved concrete surfaces. The initial plan was to test all four of these surfaces. However close examination of the pavement surface texture revealed that the basic (non-grooved) macro- and microtexture of all these four surfaces were very similar. It was therefore decided to test only two sections, one grooved and one non-grooved, identified as section C and D respectively. Section D is also used for water ingestion certification flight tests using a specially constructed water pond which can hold large quantities of water resulting in high water depths up to 13 mm and higher. During the flight testing it turned out that it was not possible to wet the grooved section sufficiently. Also large local puddles would form which could result in controllability problems when only one main wheel runs into it.

Fig. 2: NASA Wallops Flight Facility layout (source: NASA)

V. Test Procedures

A. General

All personnel were assigned duties and data collection tasks to help complete the required tests. For each test run conducted by the aircraft, run number, time of day, test-run target speed, and runway surface condition (water depth and surface temperature) were recorded along with appropriate environmental measurements such as temperature, air pressure, wind speed and direction. Measurements of the pavement surface of each test section were conducted separately from the flight tests at a later time to avoid any interference which could delay the flight tests. As the test sections experienced low utilisation by aircraft takeoffs and landings, the surface texture is not expected to have significantly changed during the period between the flight tests and the pavement surface tests. Special instrumentation onboard the aircraft recorded several parameters of interest such as speeds, accelerations, engine performance, brakes pressures, control surfaces etc.

B. Truck-wet testing

For flight tests conducted on runway sections under truck-wet test conditions, the following sequence of events and procedures were followed:

1. The test aircraft was positioned for the beginning of a run at the identified static take-off position.
2. Water trucks made three to four passes over the marked runway test section (typically 100 m long).
3. Surface water-depth measurements are collected and timed, wet surface temperature was measured.
4. The aircraft made a test run with maximum wheel braking after entering the marked test section.
5. After exiting the test section, the aircraft continued to the taxi speed by using reverse thrust and/or brakes as required after which the aircraft vacates the runway and proceeds on the taxiway at low speed to cool the brakes. The aircraft was parked at a “Cool down Zone” where brake temperatures and aircraft condition are checked by a ground engineer.
6. Surface water-depth measurements were collected and timed.

The position of the aircraft before the test section varied depending on the target entry speed into the test section. The distance before the test section is a combination of a fixed distance and variable distance (see Fig. 3). The aircraft was accelerated to the fixed distance at which the engine throttle is chopped. A fixed distance is needed to make sure that when the aircraft enters the test section the engine are running at or near idle. From a safety point of view the flight test runs could not be conducted at takeoff thrust setting together with the application of maximum braking. A low engine thrust is needed. For deriving braking friction values from the test data it is also required to have the engines running in a stable setting when the aircraft is running through the test section. Therefore an idle thrust level is preferred as this provides a low and stable engine thrust that only varies with true airspeed for a given run. Typically, turbine engines need about 5-6 seconds to spool down to idle from takeoff thrust after throttle chop. The engines could still spool down somewhat further, however, this has a small effect on the thrust produced for the time the aircraft is

in the test section. There can be a slight delay between the throttle chop and the decrease of the engine fan speed N1. The later lags the fuel flow. The distance from the test section to the engine idle point was estimated on this characteristic combined with the highest entry speeds anticipated (100-110 kts ground speed). The engine spool down is illustrated in Fig. 4 which shows a time history of the aircraft ground speed, fuel flow and engine fan speed recorded during a test run with the Citation 550. Traffic cones were set up along the side of the runway at the engine idle point and at the beginning and end of the test section. These markers were used as visual aids to the pilots in planning their actions. An example of the view on the idle point pylon from the cockpit is shown in Fig. 5. In some test runs traffic cones were also located at different position before the engine idle point.

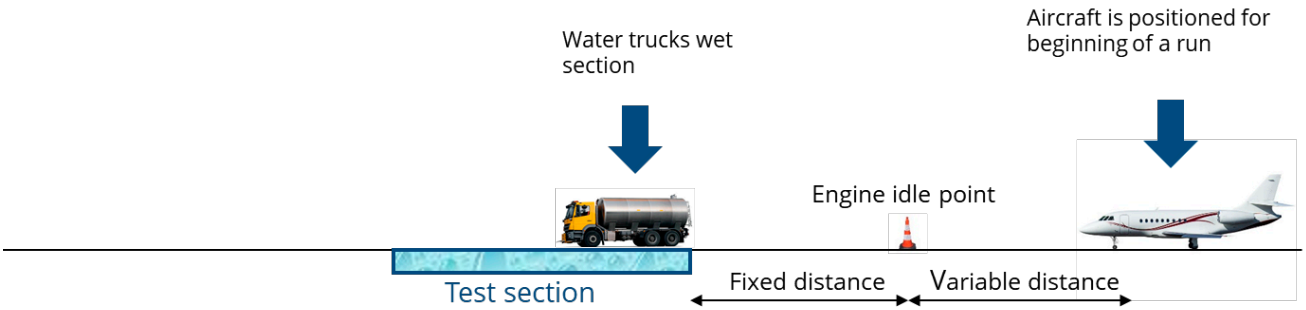

Fig. 3: illustration of the aircraft position in front of the wet test section

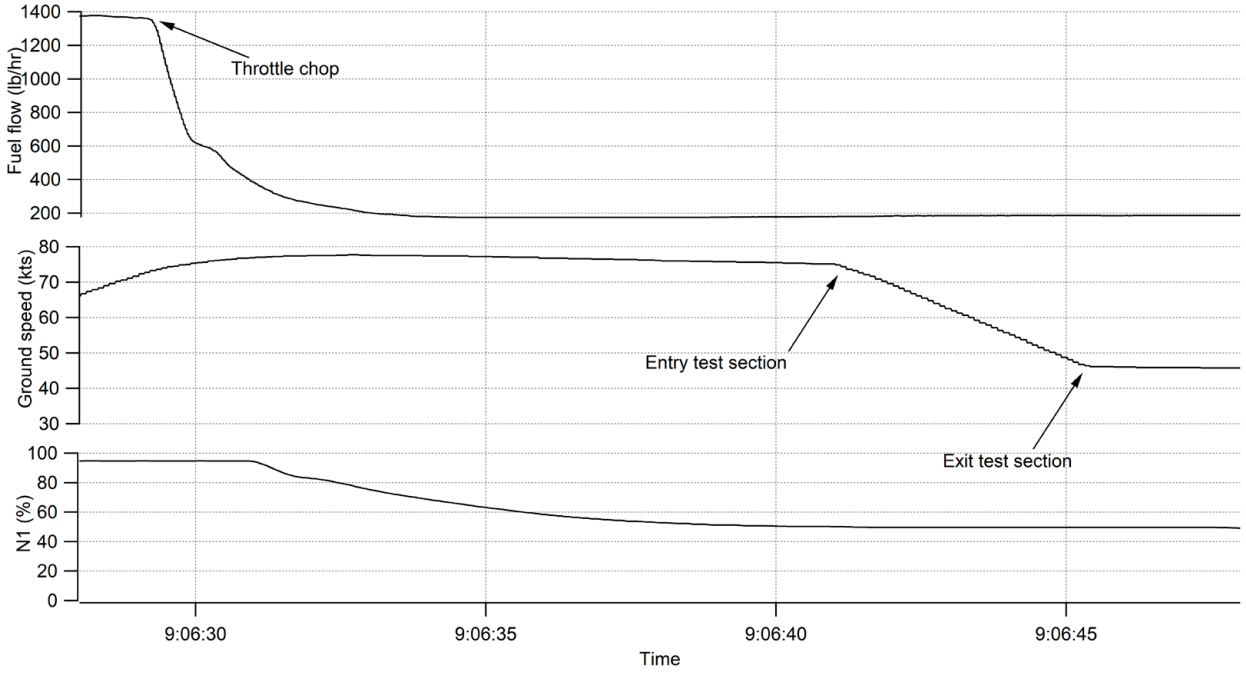

Fig. 4: Time trace of ground speed and fuel flow plus engine low pressure compressor fan speed N1 of one engine (Citation C550)

Fig. 5: example of view on the idle point pylon from the cockpit (red encircled)

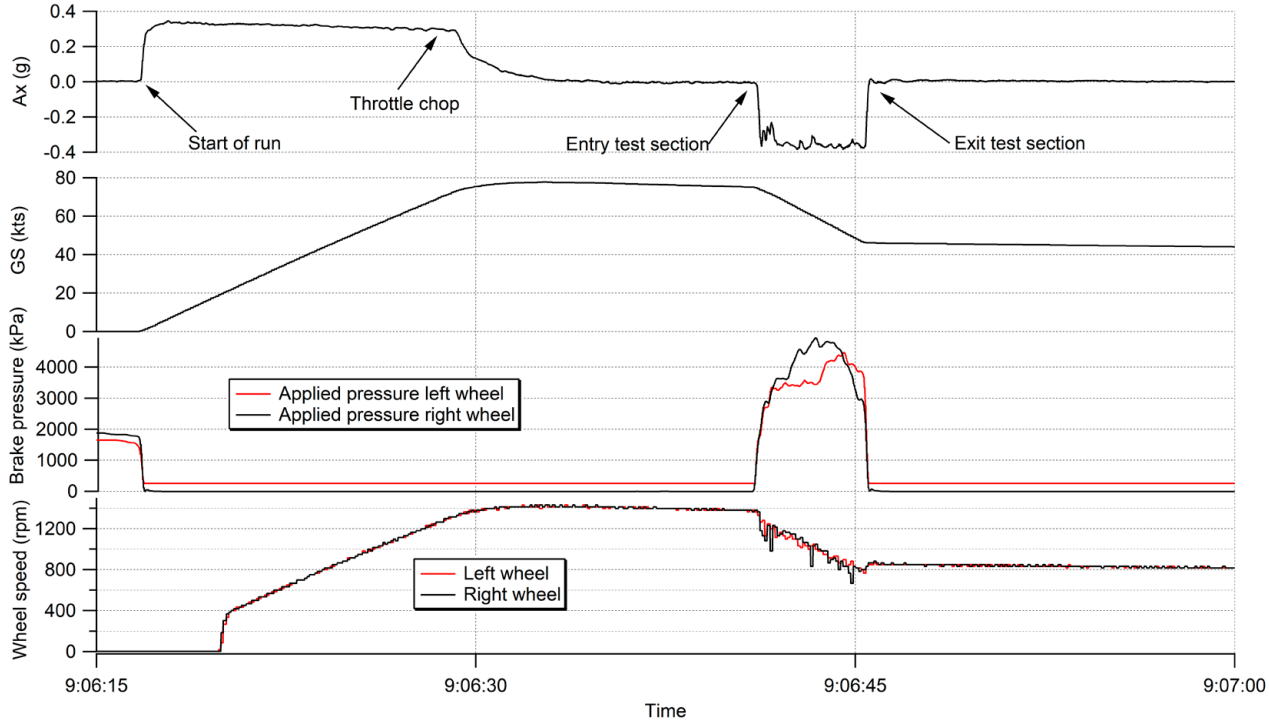

Fig. 6: example of some parameters recorded onboard during a test run as function time

An example of time histories of longitudinal acceleration, ground speed, applied brake pressure by pilots (not the antiskid), and wheel speeds[‡] recorded onboard the Citation C550 aircraft are shown in Fig. 6 for a typical test run. Also shown are the start of the run, the fuel chop, test section entry and exit.

The technique employed of artificially wetting a runway using water trucks in this study is not new. It was already described in 1962 (Ref. [2]) and applied in many other flight tests. A variety of water tanker trucks were used in this study for obtaining wet-surface conditions in the test sections. For the flight tests at the European airports, two water

[‡]Starts recording at a ground speed of approximately 20 kts.

trucks were used with a capacity of 36,000 litres and a 4.0” outlet. Water was discharged under gravity from the water trucks, on the tests section by making three or four passes (see Fig. 7). This number of passes depended on the cross slope of the test section. The two water trucks drove behind each other and discharged the water near the runway centreline. For the tests on the taxiway of Cochstedt airport the trucks were operated at a slight offset to the taxiway centreline because the taxiway was single sloped in cross direction (see Fig. 8). This approach was recommended in (Ref.[3]). The test sections at the European airports were all 100 m long. The trucks were operated at low speeds between 6-10 km/h when wetting the test section. Each truck dropped about 6,000-7,000 litres of water per run. As the outflow was by gravity the outflow rate reduced as the water tanks ran empty. Therefore the water trucks were typically refilled after 4 runs to keep a more or less consistent outflow. The outflow rate varied between 1,600-2,300 litres per minute depending on the amount of water in the tanks. Whenever the test surface was completely dry, a quick run was made with the water trucks to pre-wet the test section. This helped in filling some of the larger voids in the surface prior to the actual wetting.

The water depth levels should reflect the regulatory definition of a wet runway, e.g. any visible dampness or water up to and including 3 mm deep. For the flight tests, the target water depth was set between 0.25 and 1.5 mm which reflects water depths seen in natural rain on crowned runways. This also corresponds to the wetness seen in landing overruns. The FAA recommends that water depths should not be lower than 0.25 mm for wet runway friction tests (Ref. [4]). Previous tests conducted by the FAA and NASA showed that water depths of more than 1.5 mm are not feasible without damming as the water is drained immediately when water trucks spray the runway surface and the aircraft cannot access the runway directly after the trucks have finished spraying [5-7]. Water depths between 0.25 and 0.8 mm are more realistic to achieve without using special rubber dams in the test section. Runways surfaces with water depths of 3 mm or higher are considered to be flooded.

The tests at NASA Wallops Flight Facility were partly conducted in a water pond. This is an area surrounded by flexible rubber-belt dams that keep the water contained within that area (see Fig. 9). A groove cut 1/4 in. wide and 1 in. deep surrounds the test section and supports the rubber-belt dams. This construction allows test at higher water depths than with the truck wetting technique. After each run the water pond was refilled just prior to the start of the next run (see Fig. 10). The water pond was approximately 60 m long and 10 m wide. Additional runs were conducted without the water pond construction installed. One single water truck was then used to wet test section D in those tests as illustrated in Fig. 11. This truck had a capacity of 26,000 litres and a 4.5” gravity outlet. This was sufficient as test section D was near flat (cross and longitudinal slope 0.0 and 0.1% respectively) unlike the runways tested at the European airports which had a crowned cross section with slopes between 1.0-1.5%. The taxiway at Cochstedt was sloped in one direction (1.0%). It turned out to be too difficult to wet the grooved section C using one water truck. Even the use of an additional fire fighter truck that sprayed additional water on the grooved surface did not help. It was also noted that large water puddles formed to one side of the centreline. This would have affected the flight test results and could also affected the safety of the tests due to possible lateral control problems.

Fig. 7: water trucks wetting a test section on the runway at Braunschweig airport

Fig. 8: wetting of the taxiway of Cochstedt airport with water trucks at an offset to centreline (is yellow, solid line to the right of the truck)

Fig. 9: water pond on runway 22 at NASA Wallops Flight facility (section D)

Fig. 10: water truck ready to refill the water pond

Fig. 11: water truck wetting section D of runway 22 at NASA Wallops Flight Facility

Cooling of the brakes of the aircraft after each test run was an essential part of the test procedure. Thermal fuse plugs are mounted in the main gear wheel to prevent tire explosion caused by hot brakes. When multiple test runs are conducted without proper cooling of the brakes in between each run, heat will build-up quickly and the thermal fuse plugs will melt, deflating the tires completely. Another reason to cool the brakes is that very hot brakes will affect the braking capabilities. Once a certain total absorbed brake energy is exceeded, the brakes' ability to generate forces will diminish. Failure to properly account for this brake residual energy may result in unanticipated fade of the brakes and the inability to stop the aircraft. The lower braking force generated due to this brake fade will also result in a lower value of the braking friction coefficient derived from the test data. This can lower the average braking fiction coefficients by 30-40% (Ref. [8]). However, this is entirely the result of the brake fade and is not related to the runway surface conditions. Several strategies were employed in cooling the brakes such as active cooling using portable fans located near the wheels (see Fig. 12), use of thrust reversers after exiting the test section (only available on the Falcon 2000 test aircraft), and a single engine taxi out operation in order to reduce the taxi speeds and therefore the need to apply brakes. Only when the brake temperatures dropped below a safe value the next test run was commenced.

Fig. 12: example of active brake cooling using fans

C. Rain-wet runway testing

At NASA Wallops Flight Facility a number of tests were conducted in natural rain conditions on runway 10. These comprised of normal landings at an approach flap setting with maximum braking applied just after touchdown. An approach landing configuration was used to obtain higher ground speeds during the landing roll. For these rain-wet runway conditions, only steps 3, 4 and 5 of the test sequence were conducted. However, step 3 was taken after the aircraft had vacated the runway.

D. Water pond testing

Several runs were made in the water pond on runway 22 (test section D) at a target water depth of 1 mm. The water pond was made up of several sections separated by rubber dams installed perpendicular and parallel to the runway centreline. This is shown in Fig. 13. During one day of testing the wind was blowing water to one side of the water pond (12-17 knots from North-East direction). Furthermore, although the test section was nearly flat, there were areas that had some cross slope causing water to move into that direction also (which was the same as the wind direction). In combination with the wind isolated puddles were formed in the water pond to the right of the direction of motion of the aircraft. These can be seen in Fig. 13. Water was therefore manually moved to provide a more even water level distribution in the water pond particular at the anticipated main wheel locations. This process is illustrated in Fig. 14. Still the water levels were difficult to control and varied in the pond between 0.5-2.0 mm with some isolated areas exceeding 7 mm (mainly due to surface wind). Local water puddling, effect of surface winds, and elapsed time after water application from tanker trucks are factors which greatly influence scatter and repeatability of tire friction-measurement data in a water pond test setup.

Fig. 13: different sections of the water pond

Fig. 14: redistributing the water in the water pond

VI. Data collection and post processing

A. General

During the flight testing activities several data was collected. Both test aircraft were fully instrumented and collected several parameters during the test runs. Additionally water depth measurements using a special depth gauge were taken before and after each test run. After testing, the aircraft data was processed for calculation of the wheel braking friction coefficient. Furthermore data processing of the measured water depth data was done to model the water dissipation rate for each test section, this resulted in estimation of water depth at the time of aircraft entry into the test section.

B. Water depth measurements

Water depth measurements were obtained with the NASA water-film depth gauge at several locations within the test area that corresponded to the location of the main gear wheels in order to study the dissipation of water from the pavement surface with respect to time after wetting. The gauge is shown in Fig. 15. The gauge works on the principle of reflectivity. The instrument has a series of transparent polished Perspex rods which are set at various distances from the surface on which the instrument rests. The rods are designed such that when they are contacted by water an immediate indication of wetting is shown on the entire upper surface of the indicating rod. This is accomplished by tapering the lower end of the rod inwardly and then forming another tapered depression into the rod. When any part of the lower end of the rod is wetted, capillary action takes place drawing the liquid into the depressed area of the rod. Since water is highly reflective and will reflect more light than the runway surface, rods that are not touching the water will appear lighter than those that are touching or submerged in water. The dark rod with highest number indicates that the water depth is between this value and the next higher rod number. The NASA water depth gauge gives an immediate reading of the depth of water as it rests in position on the particular surface which is covered with water.

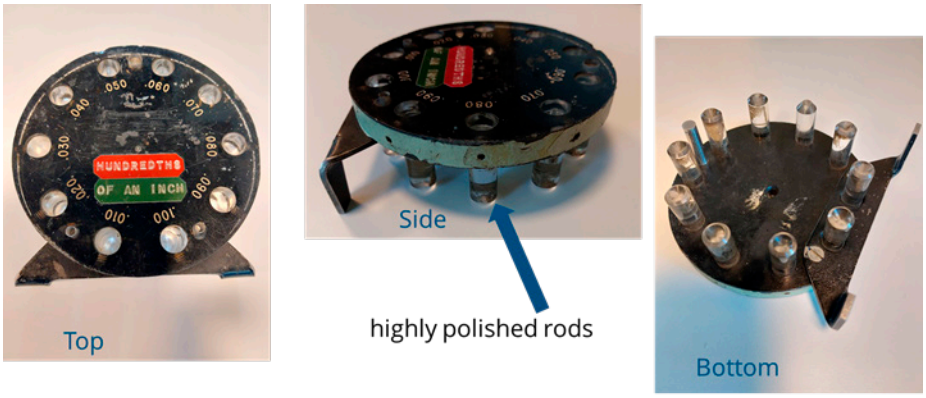

Fig. 15: NASA water depth gauge

Water on the pavement surface dissipates with time after wetting has finished due to the lateral and transversal slopes in the test section. Several water depth measurements were taken at the time the water trucks finished wetting (t=0) and after the aircraft had passed the test section. Some additional drainage tests were also conducted to capture water depths between this time range.

C. Examples of recorded data

During each test run a large number of parameters were measured and recorded. Typical parameter of interest are the longitudinal acceleration a_x, speeds (true air speed and ground speed), brakes pressures, and main gear wheel speeds. Fig. 16 and Fig. 17 gives some typical examples of the time histories of some parameters recorded during a test run.

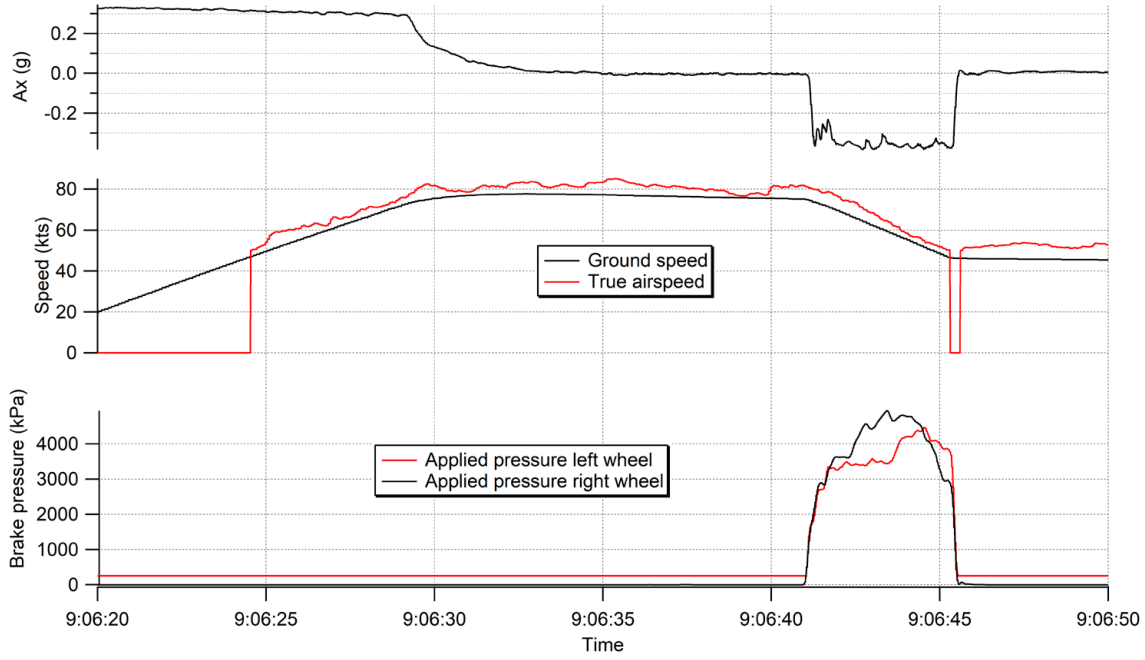

Fig. 16: Citation C550 parameter time histories and data plots obtained during test runs at Twente airport - medium speed run (target entry speed 80 kts)

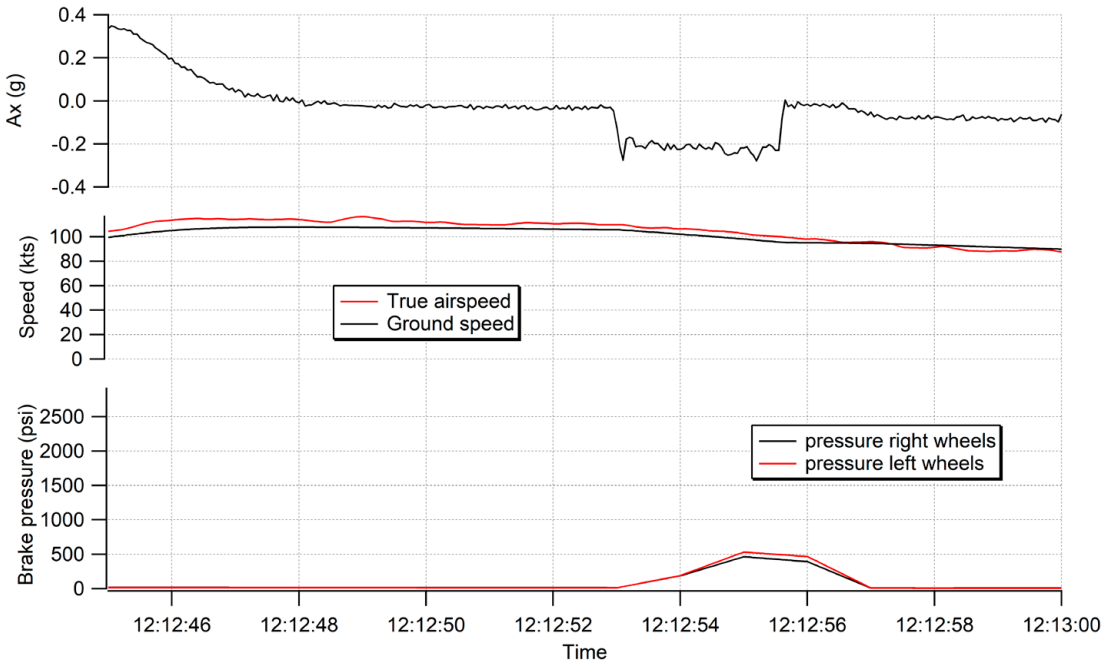

Fig. 17: Falcon 2000 parameter time histories and data plots obtained during test runs at Braunschweig airport - high speed run (target entry speed 100 kts)

D. Biases and data smoothing

Some of the recorded parameters are sensitive to biases and noise. An example of a parameter that is affected by such biases and noise is the recorded acceleration. For instance, on the Citation C550 test aircraft three independent systems record body accelerations in three directions. **Fig. 18** shows an example of the time history of the longitudinal acceleration measured in the body axis and the ground speed for the Citation C550 just before the start of the run to just at the end of the run. The acceleration shown in this example is measured by the Inertial Reference System IRS and by the Attitude and Heading Reference System AHRS. The data shown are the raw measurements which have not been filtered , smoothed or corrected for accelerometer biases and aircraft pitch angle. The measurements by the IRS are considered the most accurate and also has less noise in the recordings. The lower noise level of the IRS is also clear from **Fig. 18**. It is also visible that the acceleration as recorded by the IRS and AHRS have a small bias as both record some level of acceleration at the point that the aircraft is not moving. Partly this is caused by neglecting the pitch angle effect on the longitudinal horizontal acceleration. The bias of an accelerometer is the offset of its output signal from the actual acceleration value. This bias is somewhat higher for the AHRS than for the IRS in this example. The recorded data need to be corrected for this bias before any detailed analysis can be done. This can be partially done by correcting the acceleration for the gravitational bias due to a non-zero aircraft pitch angle. The remaining bias can be estimated by measuring the long term average of the accelerometer's output when it is not undergoing any acceleration (constant ground speed). This is the case when the aircraft is standing at its starting position on the runway. Note that the recorded ground speed also has a small bias in this example. Fig. 19 shows again the time history of the longitudinal acceleration measured in the body axis and the ground speed, however, now with corrections made for acceleration biases. Both the IRS and AHRS recorded acceleration match more closely. The AHRS longitudinal signal still shows some noise which has not been smoothed or filtered yet. Fig. 20 shows an example of corrected and smoothed longitudinal acceleration and ground speed parameter time histories.

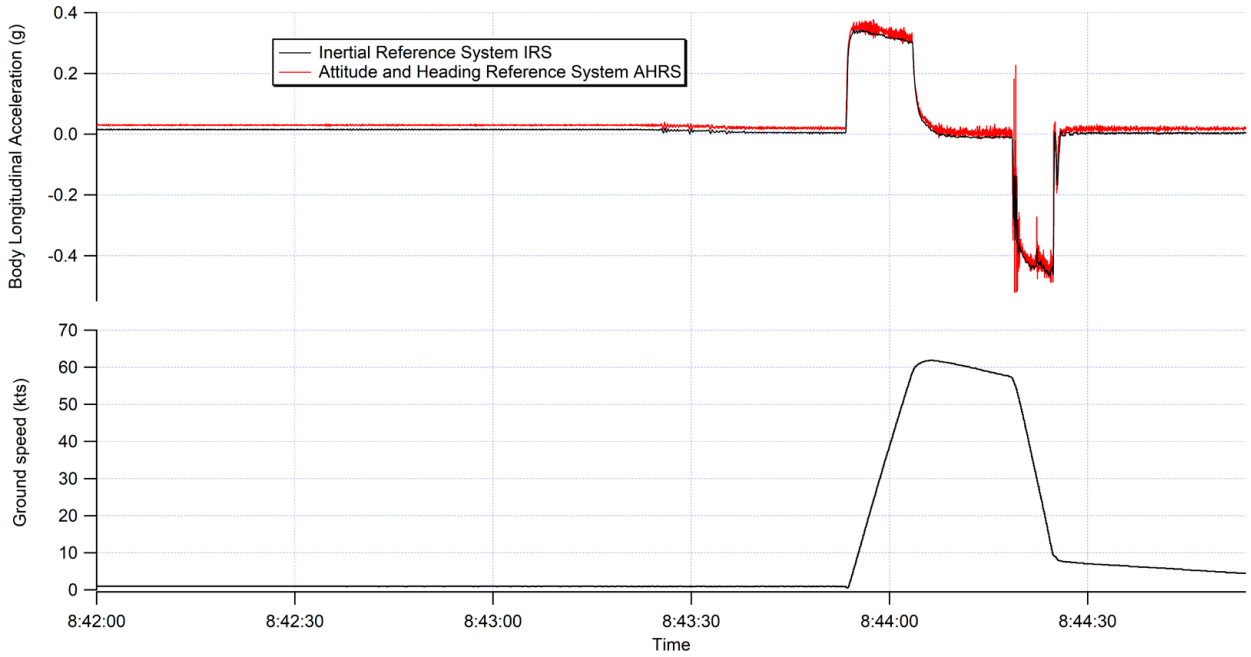

Fig. 18: example of Citation C550 longitudinal acceleration and ground speed parameter time histories (not corrected for acceleration biases or smoothed)

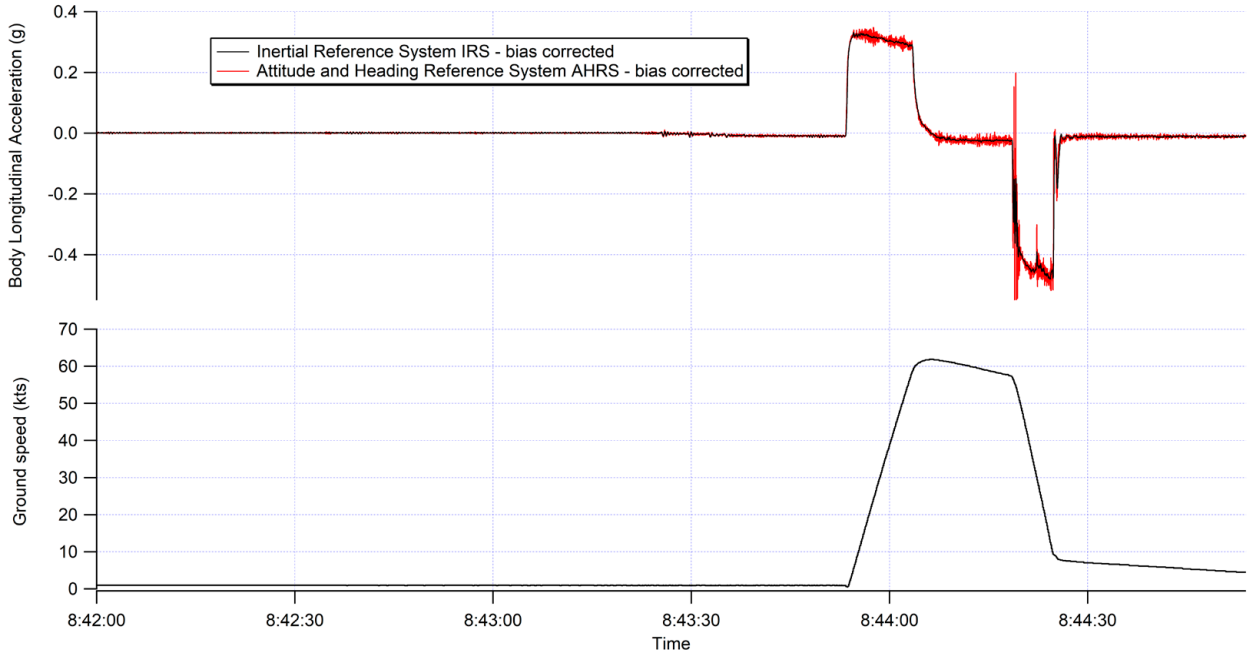

Fig. 19: example of Citation C550 longitudinal acceleration and ground speed parameter time histories (corrected for acceleration biases)

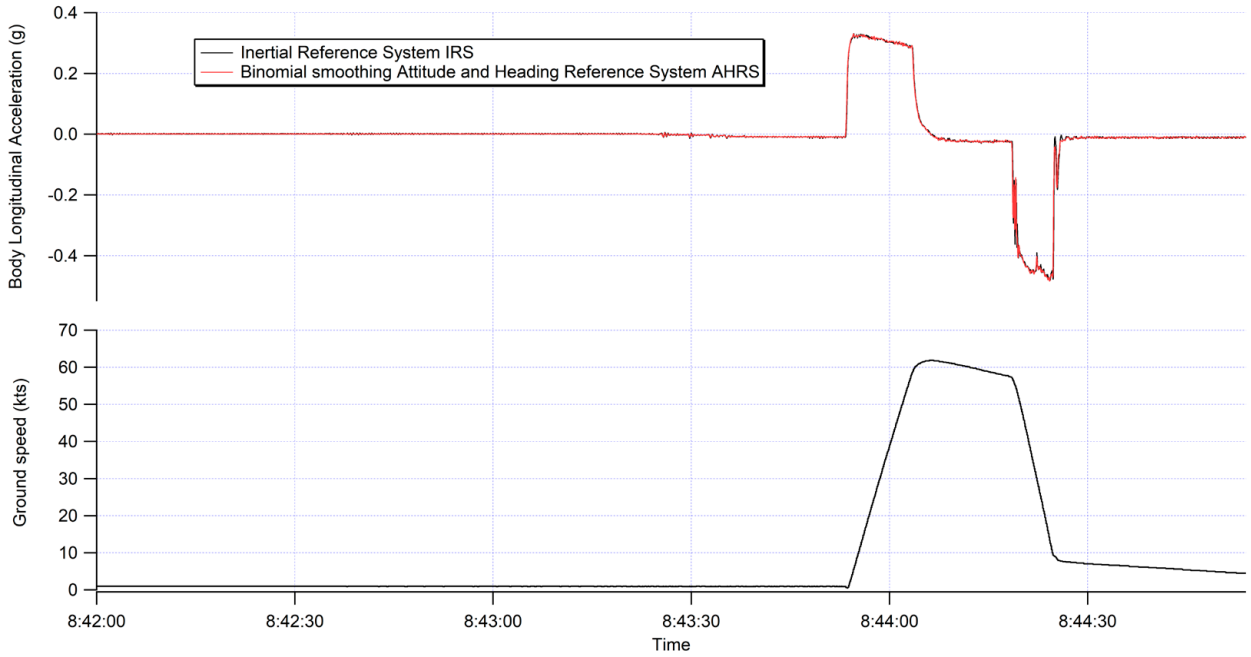

Fig. 20: example of Citation C550 smoothed longitudinal acceleration and ground speed parameter time histories (corrected for acceleration biases, AHRS signal smoothed)

E. Calculation of wheel braking friction coefficients

Ideally the determination of the braking force coefficient of the main wheels could be obtained by direct measurement of compression and drag loads on the main undercarriage legs. However, such a system is very sensitive and can introduce large errors which can be difficult to account for. Both NLR and DLR also had no previous experience in using such a test setup. Alternatively the main wheel braking coefficient of friction for each test run can be computed from the knowledge of the aircraft's aerodynamic and thrust characteristics combined with the measured onboard parameters during a braked run. This is a very common approach applied throughout the aviation industry by both aircraft manufacturers as well as research institutes. This approach is also adopted in the present study.

Fig. 21 is a free-body diagram showing the forces and moments acting on the aircraft during the braking portion of the ground roll. The lift, pitching moment, drag, and thrust forces shown can be calculated based on the recorded onboard data, the known aerodynamic and thrust properties of the aircraft, the aircraft weight, centre of gravity and ambient conditions.

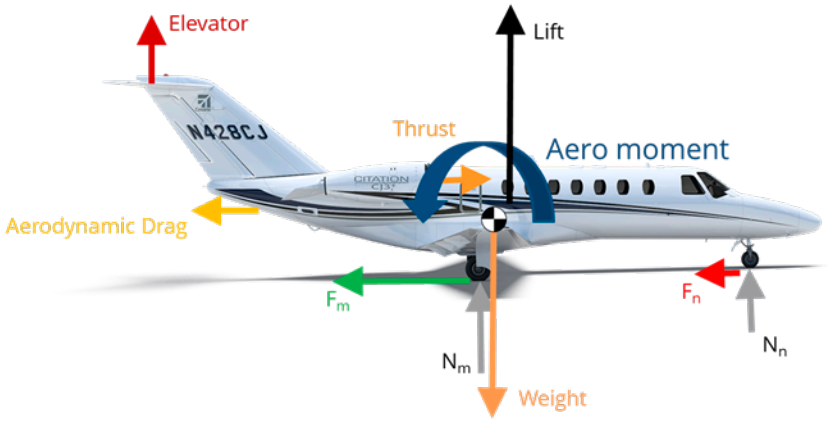

Fig. 21: free-body diagram showing the forces and moments acting on the aircraft

The vertical and longitudinal reaction forces at the main and nose gear are unknown, but can be computed by solving the system of equations representing the forces and moments acting on the aircraft.

In practice simplifications and approximations are made in the calculation of the wheel braking force from onboard recorded flight data [5, 6, 10]. One of the more simple ways for calculating braking friction coefficients is by assuming that both the nosewheel and main wheels are braking. The braking coefficient derived in this way is called the aircraft braking coefficient. The deceleration force by all the wheels is calculated from the total aircraft deceleration minus aerodynamic drag, weight and thrust components. The normal force acting on all the wheels is the aircraft weight W minus aerodynamic lift L. The aircraft braking coefficient is therefore an all-inclusive term that incorporates effects due to the runway surface, runway wetness, aircraft braking system, nosewheel rolling resistance and main gear wheels braking friction. It is therefore not the same as the main wheel tire-to-ground friction coefficient. The main gear wheel braking friction coefficient is always higher than the aircraft braking friction coefficient. However, under slippery conditions the difference between main gear wheel braking friction coefficient and the aircraft braking friction coefficient becomes smaller as it approaches the value of the nosewheel rolling resistance coefficient. The aircraft braking coefficient can be used as a validation of the main wheel braking coefficients that has been calculated using more detailed methods. The aircraft braking coefficient can be derived by summing the forces acting on the aircraft in the longitudinal direction along the runway which are then set equal to the mass of the aircraft times the longitudinal acceleration along the runway. This results in the following equation:

$$\frac{Wa_x}{g} = T_{idle} - D - W\gamma - \mu_{b\_a/c}(W - L) \qquad (1)$$

The acceleration along the runway can be calculated from:

$$a_x = a_{x\,body}\cos(\theta - \gamma) - a_{z\,body}\sin(\theta - \gamma) - gsin(\gamma) \qquad (2)$$

For the present study knowledge of the main wheel braking friction coefficient is essential which cannot be substituted by the more easily derived aircraft braking friction coefficient. The main wheel braking friction force F_m, which is equal to the normal reaction force on the main gear wheels N_m times the wheel braking friction coefficient μ_b, is also derived by summing the forces acting on the aircraft in the longitudinal direction along the runway direction which are then set equal to the mass of the aircraft times the longitudinal acceleration along the runway direction. This results in the following equation:

$$\frac{Wa_x}{g} = T_{idle} - N_m\mu_b - D - W\gamma - \mu_r(W - L) \qquad (3)$$

The normal load acting on the main wheels is calculated for a given position of the centre of gravity by balancing the lift, weight, pitching moment forces (due to the engines, elevator input and wing aerodynamic moment) and reaction force with the normal forces acting on the nose and main wheels. The contribution of the aerodynamic pitching moment and the moment induced by elevator inputs are often not taken into account in the calculation of the normal loads on the wheels.

It is assumed in the calculation of the braking friction coefficients that the brake/antiskid system is friction-limited. In this case the commanded brake pressure is greater than or equal to the brake pressure governed by the antiskid valve. The antiskid system adapts to the runway conditions by sensing an impending skid condition and adjusting the brake pressure to each individual wheel for maximum braking. In a not friction-limited condition, the wheel braking coefficient represents the level of braking applied. Uniformity in pilot brake application and proper aircraft configuration for a given series of test runs was determined from careful review of the time-history plots.

Both test aircraft used in this study are equipped with modern, modulating anti-skid systems. Each wheel is fitted with a speed transducer and its output signal is used by the anti-skid system to determine if a wheel is skidding or not. The anti-skid control valves modulates the brake pressure in proportion to the brake pedal force application. If the wheel does not skid, there is no brake pressure modulation and the brake pressure corresponds to the pedal position. When the onset of skidding is sensed, the anti-skid control valve is commanded to release its brake pressure allowing the wheel to momentarily rotate freely. The anti-skid control valve then allows the brake pressure to build up again, until the wheel skids again. After that the valve starts to reduce the brake pressure again, to a lesser degree than previously, until the wheel no longer skids. This iterative process takes a short amount of time, during which the

braking friction force between the pavement and tire is less than maximum (typically at frequency of 200 Hz). The system is then running in its anti-skid limited region providing the most optimum braking capabilities. The anti-skid brake system automatically disengages when ground speed falls below a certain value (for instance approximately 12 kts for the Citation C550).

Any change in runway friction will cause the system to adapt to these changes and begin the iterative process again. If the friction suddenly reduces, the system has to adjust the anti-skid control valves to the new friction level by reducing the brake pressure. After this the iterative process begins again. Anti-skid system response to transient runway conditions has been investigate by NASA (Ref.[11]). This NASA research showed that upon entering a wet pavement with brake pressure already being applied, the wheels can rapidly decelerate to a deep skid. This is noted by the immediate reduction in wheel speed. The flight tests in this study were conducted on partly wetted runway surfaces (as to be discussed later in more detail). If braking started just before entering the wetted test section (which cannot be ruled out), a deep skid might occur when the wheels enter the wet pavement. As a result the wheel speed could drop with the anti-skid reacting by reducing the brake pressure. The anti-skid system has to adjust the anti-skid control valves by reducing the brake pressure. This would be visible in the test data by a momentarily reduction in deceleration of the aircraft which coincides with the beginning of the wetted area on runway.

At high normal wheel loads (e.g. when the aircraft is heavy and running at low speeds) on a rough (e.g. dry) pavement surface, the wheel braking force may become limited by the maximum torque the brake system can generate. Torque-limited refers to the situation where for a given pressure, the brake torque is insufficient to cause a spin-down of the tire. In that case skidding is essentially not possible and therefore no anti-skid cycling occurs and the aircraft is not operating anymore in the anti-skid limited region. A close examination of the wheel-speed time history should show sufficient variations in both magnitude and frequency to demonstrate that the brake is not torque-limited [Ref. (11)]. This requires a sufficiently high sample rate of the recorded wheel speed. During the flight tests conducted in this study such high frequencies could not be measured due to limitations of the installed data sensors. Wheel speeds could not directly recorded from the anti-skid data bus. Torque-limited braking conditions occur at high wheel loads combined with high braking forces. The aircraft in this study were tested at low weights to reduce the normal main gear wheel loads which reduces the likelihood torque-limited conditions.

The test aircraft are equipped with a locked wheel crossover protection that prevents loss of control caused by unequal wheel rotation rates. When the anti-skid system detects that one main gear wheel is rotating 50% slower than the other, brake pressure to the slow wheel is dumped, allowing wheel speeds to equalise. Locked wheel crossover protection is functional at ground speeds greater than 40 knots for the Citation C550.

F. Aircraft performance model validation

An aircraft performance model determines the forces acting on the aircraft based on the current state of the aircraft (e.g. flaps setting) and the ambient conditions. The aircraft performance models used are based on information provided by the aircraft manufactures. These models include details on the installed engine thrust, aerodynamic characteristics of the aircraft (lift, drag, pitching moment), and wheel rolling resistance. These models are so-called point mass models referenced around the centre of gravity. Although these models have been validated by the aircraft manufacturers some checks were conducted to ensure the correctness of their implementation and the accuracy of the data acquisition systems used in the flight tests.

VII. Results

A. Water Depth Measurements

An example of the water depth measurements on the test section of the runway at Braunschweig airport is shown in Fig. 22. Similar measurements were taken at each test location. Also shown are the times at which the aircraft passed the test section. This allows the derivation of an interpolated value of average test section water depth at time the aircraft was in the test section. An overview of the estimated average water depths during time the aircraft passed the test section are listed in Table 1.

Table 1: estimated range of water depths at time of aircraft passing

Location	Water depth mm
Cochstedt taxiway	0.80-0.95
Cochstedt runway	0.70-0.90
Braunschweig	0.65-0.80
Twente	0.70-0.80
Wallops section D	≈1.00*

**puddles present to the right side of the centre line in direction of flight.*

The level of scatter found in the measured water depths in this study is consistent with previous tests in which the same type of water depth gauge was used (see Ref. [5] and [7]). The scatter in the measured water depths can be caused by a variety of factors such as the resolution of the gauge itself, surface wind, grease on the rod faces, and operator use. Note that the faces of the rods were degreased before each use. The readings are furthermore affected by the positioning of the three supporting prongs with respect to possible irregularities in the runway pavement surface. Care was therefore taken were to position the water depth gauge. The depth gauge was also oriented in different ways with respect to the runway when depth measurements were taken. Test section D on runway 22 of Wallops Flight Facility showed local areas with puddles right to the centre line in the direction of flight. These puddles can affect the achieved braking levels and the behaviour of the antiskid system.

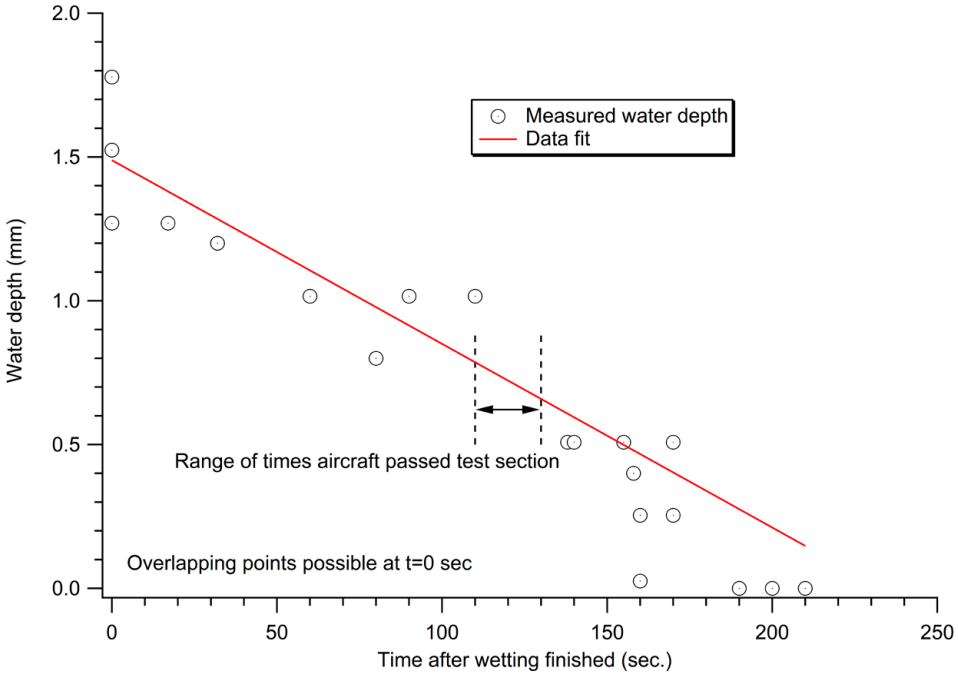

Fig. 22: Measured water depth as function of time after wetting finished – runway Braunschweig airport

The wetness of the surface can vary along the test sections particular for those having a large cross slope (except section D at NASA Wallops which was near flat) due to runoff that starts immediately after the water trucks passes. This could have some effect on the measured deceleration as wheel braking friction forces are influenced by water depth. In the test program, the last pass by the water trucks was always opposite to the direction of travel of the test aircraft which allowed more time for water runoff at the end of the test section than at the beginning (except for the tests on section D at Wallops). This problem of uneven wetness is typical to all flight tests that used water trucks to artificially wet the runway. However, little attention has been given to the issue. It was mentioned in a study done by Douglas Aircraft Company for the Federal Aviation Administration [3,9]. As said it is difficult to achieve an evenly

wetted test section when the water trucks all travel in the same direction and the test section is relatively long, as water laid at the start will drain away by the time the trucks reach the end of the test section. Running trucks in opposite direction could help to minimise the unevenness in water depth (Ref. [3]). However, in this situation it is more difficult to coordinate the trucks. Also the time required to clear the runway after wetting has finished could increase using this way of operating the water trucks. However, even with this approach of opposite truck movements it is still hard to achieve an evenly wetted test section. To minimise the described effect the test section was kept relatively short (60-100 m) in this flight test program compared to other tests done in the past which used test section which were ten to twenty times longer. No water depth measurements were made at the very end or beginning of the test section during this study. However, video images from the GoPro recordings made from the cockpit suggest (see e.g. Fig. 23) that only near end of the test section the area was drying up somewhat at the anticipated wheel location. In Fig. 23, the actual wheel position makers used for the water depth measurements on the runway are visible left and right of centreline (double yellow lines). These locations have been extrapolated towards the end of the test section to show the level of wetness that can be seen (dashed line). The dashed line is added to the picture only for illustration purposes. It was not marked on the runway itself.

Fig. 23: cockpit view on wet test section (dashed lines added for illustration purposes and not visible to the pilots)

Two landings were conducted on runway 10 of NASA Wallops Flight Facility with the Citation C550 aircraft. Water depth on the surface at several locations along the runway was measured right after the aircraft had landed. After the first landing, water depths were measured between 0.5 and 1.0 mm with most readings at 0.5 mm. Fig. 24 shows the runway just after the first landing. Rain was falling at this time which can been seen by the black spots on the wetted area of the runway. During the second landing the rain intensity was less than during the first landing. The runway conditions at the main gear wheel location varied from damp (0.00-0.25 mm) to wet (0.25 mm). In some areas along the runway, 0.5 mm of water depth was measured.

Fig. 24: rain-wet runway 10 of NASA Wallops Flight Facility

B. Wheel Braking Coefficients

Fig. 26 through Fig. 28 give some examples of the wheel braking friction coefficients as function of ground speed derived from the different test runs conducted on each runway. The friction levels and its variation with ground speed vary between the different tests due to differences in macro and micro texture of the surfaces. Also the main gear tires if the Citation C550 and Falcon 2000 have different inflation pressures (115 psi versus 225 psi) which also affects the friction levels on a wet runway surface. Fig. 25 gives an example of the wheel braking friction coefficient as function of ground speed and the aircraft braking friction coefficient. As discussed the latter is an all-inclusive term that incorporates effects due to nosewheel rolling resistance. It is therefore not the same as the main wheel tire-to-ground friction coefficient. However as its computation requires much less details it can be used as an overall verification of the friction levels found from the computed main wheel braking friction coefficients.

On the Citation C550 aircraft bias-ply type tires are installed on the main landing gear. On the Falcon 2000 radial-belted tires are used. Radial-belted tires are the most modern design of aircraft tires. Radial-belted aircraft tires differ to bias-ply aircraft tires in that the plies all run radially from bead to bead at approximately 90° to the centre-line of the tire. Angled belt plies are laid between the tread and the top casing ply, resulting in a flatter tread and adding strength to the tire. Test data show that radial-belted aircraft tires provide very similar braking friction characteristics on both dry and wet runways compared to bias-ply tires (Ref. [12]) for tires of the same size and inflated to the same pressure for a range of ground speeds from 60 to 160 kts. The only known difference is that radial-belted tires have a lower dynamic hydroplaning speed than bias-ply tires (Ref. [13]). This can affect the braking friction levels on flooded and slush covered runways. Also surfaces with a very smooth macro texture can show lower friction levels for radial-belted tires on wet runways.

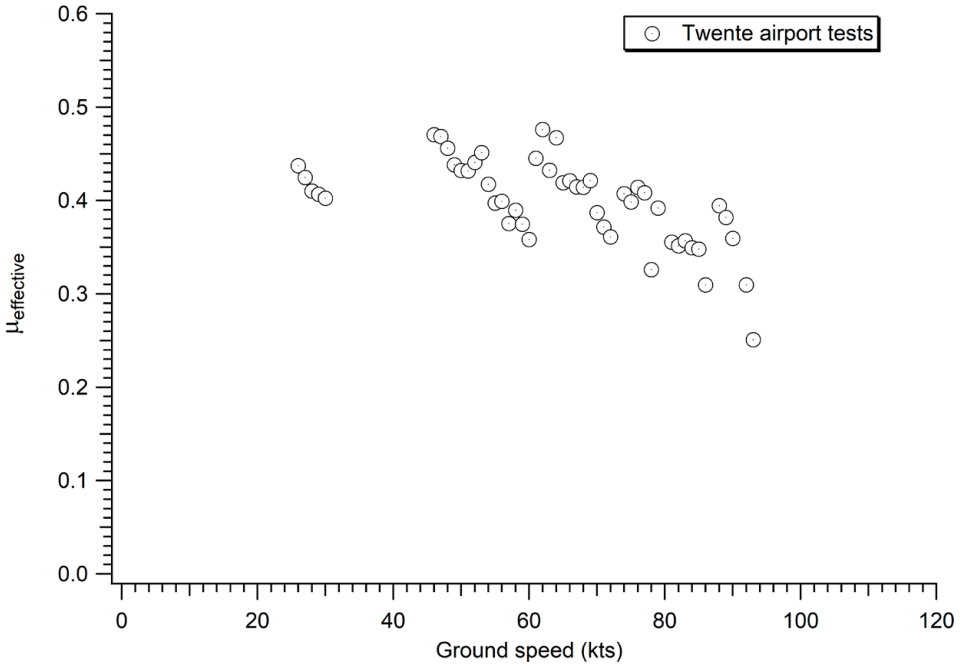

Fig. 25: variation of Citation C550 effective braking friction coefficient with ground speed for wet runway tests at Twente airport

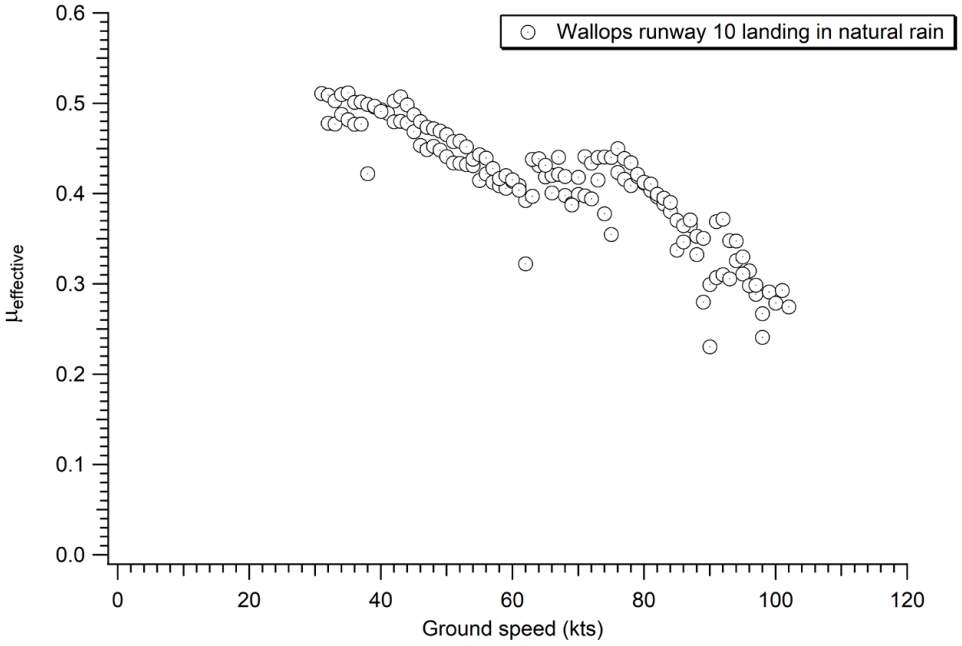

Fig. 26: variation of Citation C550 effective braking friction coefficient with ground speed for wet runway tests at Wallops airport runway 10

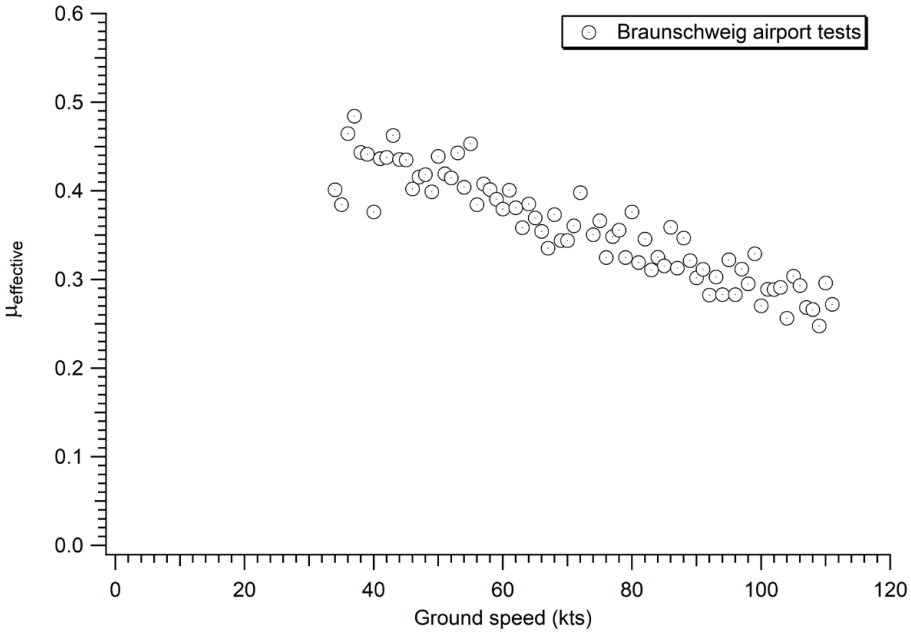

Fig. 27: variation of Falcon 2000 effective braking friction coefficient with ground speed for wet runway tests at Braunschweig airport

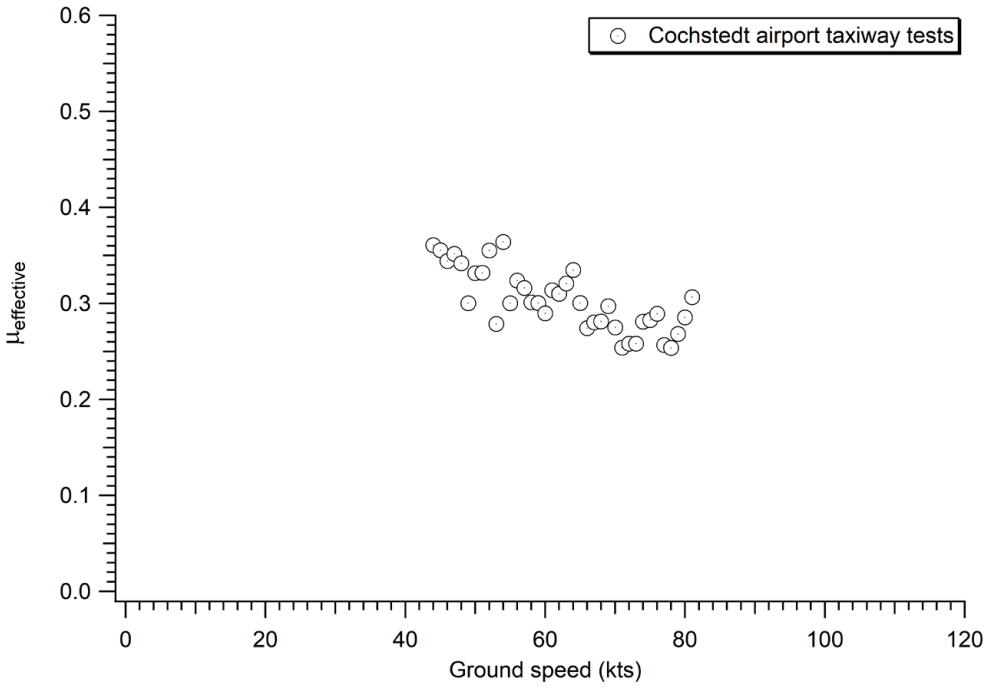

Fig. 28: variation of Falcon 2000 effective braking friction coefficient with ground speed for wet runway tests at Cocohstedt airport (taxiway)

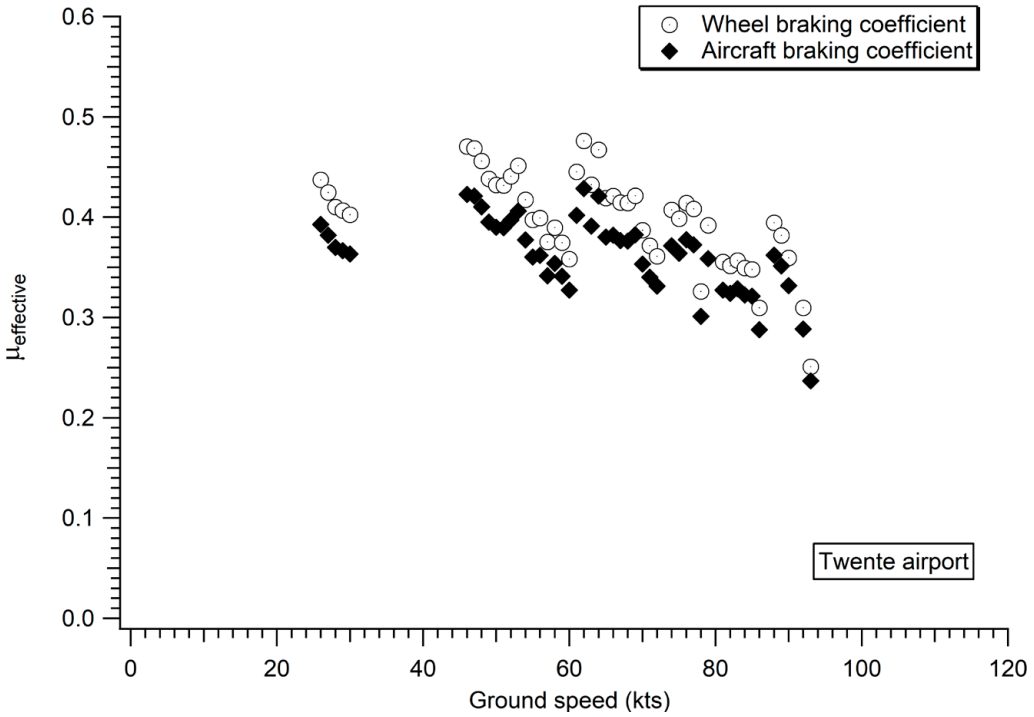

Fig. 29: comparison of the variation of Citation C550 effective braking friction coefficient with ground speed for wet runway tests at Twente airport

C. Aircraft Performance Model Validation

Comparisons were made between the longitudinal acceleration predicted by the performance model and tare runs (with the wheels unbraked and the engines running at idle). The sum of the aerodynamic, propulsion, and other forces should equal the measured deceleration force. An example of a comparison between the aircraft model and a tare run is shown Fig. 30. Also comparisons with braking friction coefficients derived by the aircraft manufacturers on dry runways were made (see for instance Fig. 31).

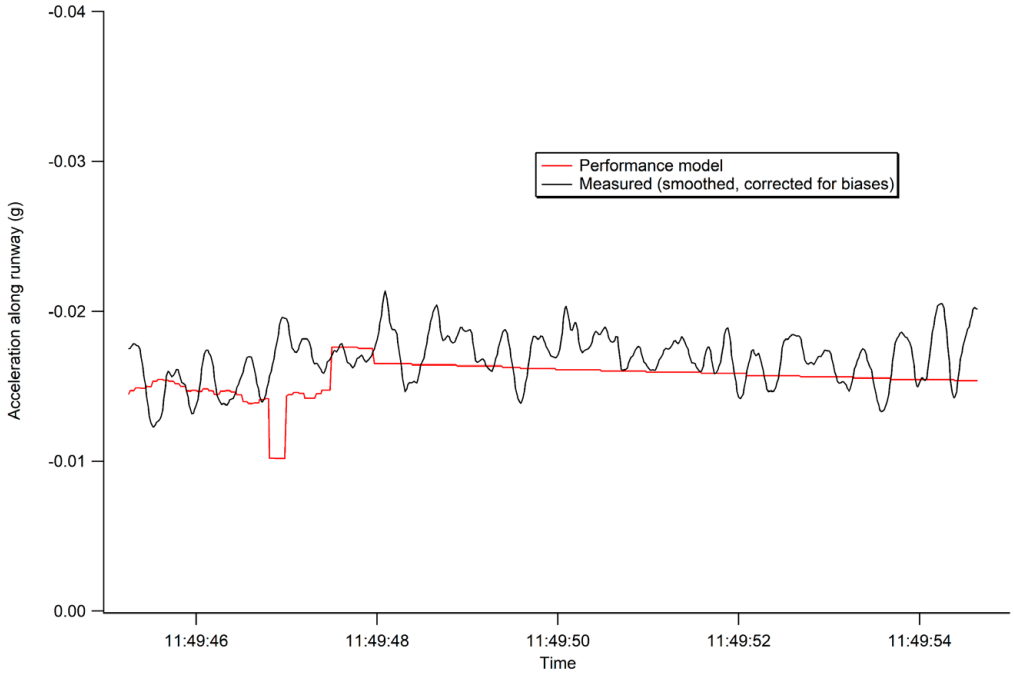

Fig. 30: comparison between performance model predicted and measured longitudinal acceleration in an unbraked condition (Citation C550)

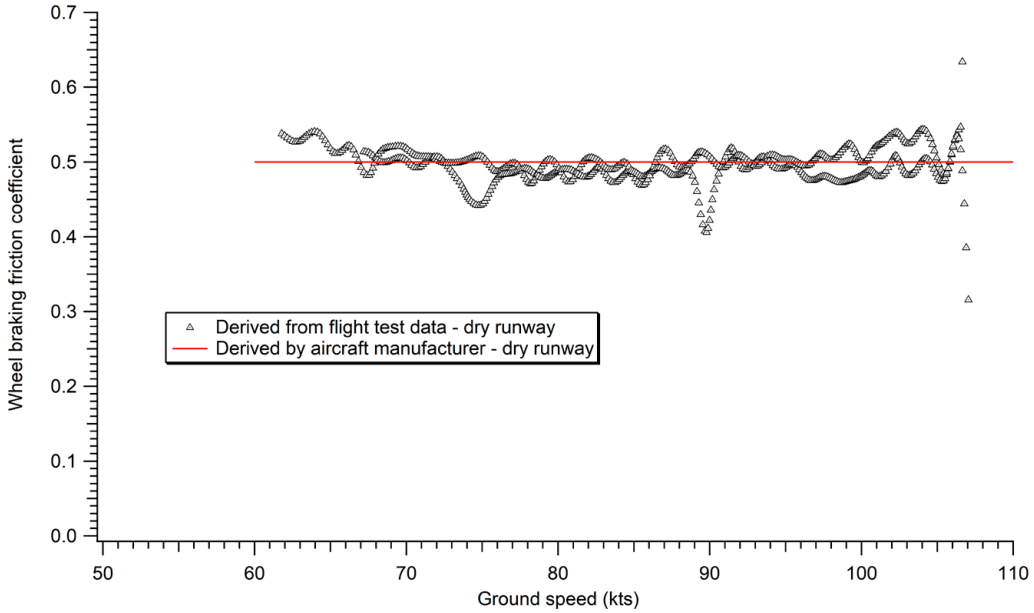

Fig. 31: comparison of dry wheel braking friction coefficients as function of ground speed derived in the current flight tests and by the aircraft manufacturer (C550 aircraft)

VIII. Conclusions and further activities

This paper presented several test activities that were part of an EASA project conducted by NLR and its partners DLR and ESDU for the characterization of aircraft braking friction on wet runways. The objective of the project is to address the risk of overruns caused by deficiencies in runway micro texture, and explore the use of laser-scanning to

establish suitable thresholds for runway surfaces which define when a runway is slippery when wet. The test campaign included several high-speed ground test runs on wet runways with two fully instrumented test aircraft. By means of these test runs, the aircraft braking performance can be determined. Further activities include analysing the correlation between the braking friction coefficient and the runway microtexture.

For the flight tests, the target water depth was set between 0.25 and 1.5 mm. By taken several water depth measurements at given time intervals at each test section, the water dispersion rate could be characterized per testing location as a function of time. By doing so, the range of water depths at time of aircraft passing could be estimated per testing location. The range of water depths during the testing campaign at the time of aircraft passing through the test section ranged from 0.65 mm – 1.00 mm.

Onboard recorded parameters like aircraft accelerations and speed were used to calculate the braking friction coefficient. For this purpose a performance model was used that comprising of the thrust and aerodynamic characteristics of the aircraft. The results will be used to analyse the effects of macro and micro texture on the wet runway braking characteristics in a later part of the project.

The testing activities of this project were not limited to flight testing activities. Surface measurements have been conducted using a high-resolution laser scanner and a British Pendulum Tester. Data from these surface tests will be analysed in conjunction with the calculated wheel braking friction to determine the effect of micro texture on aircraft braking action. Furthermore, next steps in the project will also include establishing threshold values for runway surfaces which define when a runway is slippery when wet. These thresholds will be based on the data that was gathered during the extensive testing campaign that were described in this paper.

Acknowledgments

The work presented in this paper is conducted under contract with the European Union Aviation Safety Agency EASA. This project is fully funded from the European Union's Horizon Europe research and innovation programme.

References

[1] Anon., “Annual Safety Review 2023,” European Union Aviation Safety Agency, 2023. doi: 10.2822/83672

[2] Keyes, H., “A Review of the Problems of Aircraft Wheel Braking on Wet Surfaces and a Description of a Method of Artificially Wetting Runways for Test Purposes”, Ministry of Aviation, Aeronautical Research Council Current Paper 592, London, UK, 1962.

[3] Beaty, I., and Sugg, R., “Trials to compare the stopping performance of three antiskid systems and to demonstrate methods of determining aircraft stop distances on the standard military reference wet surface”, Procurement Executive, Ministry of Defence, S & T-Memorandum-3-79, October 1979.

[4] Anon.,”Measurement of Runway Friction Characteristics on Wet, Icy or Snow Covered Runways”, Federal Aviation Administration FAA, Report FS-I60-65-68-I, FAA, Washington DC, 1971.

[5] Horne, W., Yager, T., Sleeper, R., and Merritt, L., ”Preliminary Test Results of the Joint FAA-NASA Runway Research Program, Part I—Traction Measurements of Several Runways Under Wet and Dry Conditions with a Boeing 727, a Diagonal Braked Vehicle, and a Mu-Meter”, NASA Technical Memorandum TM X-73909, NASA, Langley Research Center, Hampton, Va., 1977.

[6] Merritt, L., “Concorde Landing Requirement Evaluation Tests”, Federal Aviation Administration FAA, Report FS-160-74-2, FAA, Washington DC, 1974.

[7] Yager, T., Vogler, W., Baldasare, P., ”Evaluation of two transport aircraft and several ground test vehicle friction measurements obtained for various runway surface types and conditions. A summary of test results from joint FAA/NASA Runway Friction Program”, NASA TP-2917, Langley Research Center, Hampton, Va., 1990.

[8] Schofield, L., “Equations and Techniques for Computing Braking Friction Coefficients and Braking Energies”, FTC-TIM-71-1003, Air Force Flight Test Center, Edwards AFB, California, May 1971.

[9] Preston, O. W., Kibbee, G. W., Muroyama, R. H., Storley, R. A., “Development of a Basic Methodology for Predicting Aircraft Stopping Distance on a Wet Runway”, Federal Aviation Administration, Report FAA-RD-70-62, FAA, Washington DC, 1971.

[10] Doogan, M. Herrmann, E. and Lamont, P., Braking friction coefficient and contamination drag for the Dash 8 on winter contaminated runways, de Havilland Inc., Report DHC-D4547-97-09, 1997.

[11] Tanner, J. A., Stubbs, S. M., and Smith, E. G., “Behavior of aircraft antiskid braking systems on dry and wet runway surfaces: Hydromechanically controlled system”, NASA TP-1877, NASA Langley Research Center Hampton, VA,, 1981.

[12] Yager, T., Davis, P., Stubbs, S., and Martinson, V., "Braking, Steering, and Wear Performance of Radial-Belted and Bias-Ply Aircraft Tires," SAE Technical Paper 921036, 1992, doi 10.4271/921036.

[13] Van Es, G.W.H., “Hydroplaning of modern aircraft tires”, National Aerospace Laboratory NLR, Technical Paper 2001-242, Amsterdam, 2001.